Control of the width of active Western Antarctic Siple Coast ice streams by internal melting at their margins

Thibaut Perol,[1,2] and James R. Rice[2,3] (submitted to JGR - F, 20 July 2012)

Abstract. Why do ice streams exist on the Western Antarctic Ice Sheet, like near the Siple Coast? And what sets their width? They are streams of typically 30-80 km horizontal width, flowing rapidly towards the Ross Sea at hundreds of m.yr^{-1}. The streams are bordered by slow moving ice, frozen to the bed, but no structure in the bed has been cited as controlling the location of the stream margins. We examine, and find evidence supportive of, the hypothesis that the stream width is set by the development of significant internal melting, i.e., development of temperate ice conditions, within the sheet. We first show, from published ice sheet deformation data and from thermal modeling based on temperature-dependent flow and conduction properties, that most existing Siple Coast ice stream margins are indeed in a state of partial melt, with temperate ice being present over a substantial fraction of the sheet thickness. We then propose and quantify approximately, if incompletely, a possible related mechanism of margin formation, that is, of locking the sheet to the bed outboard of that temperate zone. Shear heating of the temperate ice continually generates melt which percolates toward the bed below. If that develops a channelized marginal drainage of Röthlisberger type, standard theory argues that the high, nearly lithostatic, pore pressure elsewhere (i.e., near the bed within the fast moving stream) is somewhat alleviated within the channel. That results in a higher Terzaghi effective normal stress, which we quantify approximately, acting along the bed just outboard of the channel, and hence creates high resistance against frictional shear and locks the ice outboard to the bed, naturally forming an ice stream margin. Our estimates are that the effective normal stress acting on the bed just outside such a channel is nearly two orders of magnitude larger than that inferred to be present at the bed within the fast-moving stream.

1. Introduction

Complete collapse of the West Antarctic ice sheet would raise global sea level by around 5 m [*Vaughan and Spouge*, 2002]. Siple Coast Ice Streams (SCIS) in West Antarctica drain into the Ross Ice Shelf a large amount of ice at speeds of hundreds m.yr^{-1} (about 2 to 3 orders of magnitude higher than the surrounding ice [*Brocq et al.*, 2009]). The evidence of recent and rapid changes of stream flow rates within a few decades [*Shabtaie and Bentley*, 1987; *Joughin et al.*, 2005] might have a significant effect on sea-level over time-scales of centuries. Because the width of the rapid flowing ice may control the net mass flow rate [*Van Der Veen and Whillans*, 1996], we focus this work on identifying the mechanism that sets stream margins where they are, studies on which a preliminary report is given by *Perol and Rice* [2011].

Ice streams are about 1 km thick, active along hundreds of km, are typically 30 to 80 km wide and have low surface slope ($\sim 1.3\times10^{-3}$ [*Joughin et al.*, 2002]). Ice flow is driven by a relatively small gravitational driving stress ($\sim$ 10 kPa), thought to be accommodated primarily through basal drag and laterally shear stressed zones at the margins [*Whillans and Van Der Veen*, 1993]. They are underlain everywhere by a Coulomb-plastic bed with an extremely low yield strength ($\sim$ 1 to 5 kPa [*Kamb*, 2001]), which is determined by the water content of the till (in which fluid pore pressure is close to the ice overburden pressure) and is independent of strain rate [*Tulaczyk et al.*, 2000]. Since basal sliding occurs beneath ice streams, it is appropriate to equate basal shear stress to the yield stress and hence most of the resistance to the driving stress is accommodated by side drag [*Joughin et al.*, 2004a] and elevated basal shear stress just outside the shear margins where the till is frozen [*Raymond et al.*, 2001].

The margins play an important role in the force balance of an active ice stream and have been subject of numerous studies the past two decades, especially the estimation of their side drag in order to quantify in which proportion they support the downslope weight. Detailed analysis of transverse velocity profiles across streams using analytical and numerical models of ice flow have shown that ice cannot have uniform properties across the ice stream. At margins where the shear strain rate is high, the ice should be warmer and thus weaker than in the center (e.g., *Echelmeyer et al.* [1994] for Whillans ice stream and *Scambos et al.* [1994] for Bindschadler ice stream). Using the shear strain rate profile (extracted from the shape of the velocity profile), a stress-equilibrium in the downstream direction neglecting the longitudinal stress gradient and considering the lateral shear strain rate as uniform over depth, they attempted to adjust the distribution of basal drag across the stream to keep it positive. Such was found to be not possible when the temperature-dependant creep parameter A of Glen's law, $\dot{\epsilon}_{ij} = A\tau_E^2\tau_{ij}$ [*Cuffey and Paterson*, 2010], is assumed to be laterally homogeneous (i.e., when A is constant in the transverse direction). Both *Scambos et al.* [1994] who allow A to vary with depth according to an input temperature profile and *Echelmeyer et al.* [1994] who set A to be vertically uniform at its value for -15 $^\circ C$, are able to fit the strain

[1]École Normale Supérieure, département des Géosciences, Paris, France.

[2]Department of Earth and Planetary Sciences, Harvard University, Cambridge, Massachusetts, USA.

[3]School of Engineering and Applied Sciences, Harvard University, Cambridge, Massachusetts, USA.

0148-0227/12/$9.00

rate profile only by introducing an enhancement factor E in Glen's law ($\dot{\epsilon}_{ij} = EA\tau_E^2\tau_{ij}$) that varies laterally. This factor illustrates lateral softening close to the margins due to such factors as shear heating or oriented ice fabric developed by large accumulation of shear strain. Since *Jackson and Kamb* [1997] have sampled the ice where *Echelmeyer et al.* [1994] invoke large softening (i.e., E large) and have not found a strongly developed single maximum fabric that would be expected in such shear zone (i.e., a fabric with c-axis oriented normal to the lateral shear plane), we explore the role of shear heating on the mechanism of margin weakening.

In this paper we use a 1-D conduction-advection heat transfer analysis that predicts the vertical distribution of T, and hence $A(T)$. Rather than uniformly increasing A by a fitted E as in *Scambos et al.* [1994], we incorporate the internal shear heating from lateral deformation of ice in the heat transfer analysis to find the thermal regime at the margins and ultimately derive a more accurate vertical distribution of the creep parameter that allows us to evaluate the side drag.

We investigate that thermal regime for active well-developed shear margins of Siple Coast ice streams. From published ice sheet deformation data [*Joughin et al.*, 2002] and thermal modelling, we find that most margins are in a state of partial melt with temperate ice present over a substantial fraction of the sheet thickness adjoining the bed. This concept accords with previous modelling studies of strain heating in a representative shear margin [*Jacobson and Raymond*, 1998], which suggested that a core of temperate ice within a shear margin can extend vertically as much as several hundred meters. Shear heating of temperate ice continually generates meltwater at ice grain interfaces and percolates toward the bed below via a vein and node system described by *Nye* [1989] in polycrystalline ice. Using the example of the south margin of Whillans ice stream B2 we quantify this meltwater supply along the bed and suggest that it could cause the development of a marginal channelized drainage of Röthlisberger type. Standard theory argues that the high, nearly lithostatic, pore pressure near the bed within the fast moving stream is somewhat alleviated within the channel, which operates at reduced water pressure [*Röthlisberger*, 1972; *Nye*, 1976]. That results in a higher Terzaghi effective stress just outboard of the channel which plausibly locks the ice to the bed, naturally forming a limit to the width of the stream of fast-flowing ice. This paper examines the hypothesis that internal melting at margins is the process that controls the width of active Siple Coast ice streams.

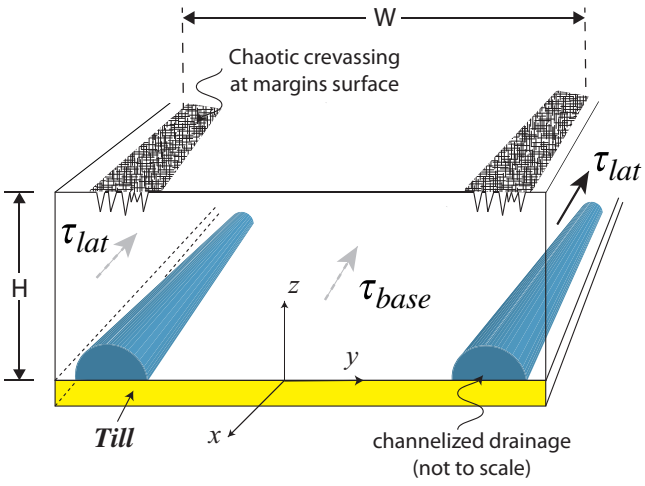

Figure 1. Sketch of a Siple Coast ice stream cross section. Ice thickness H greatly exaggerated relative to stream width W; typically $W/H \sim 30$ to 85 for ice streams and $\sim$ 10 to 20 for their tributaries. The ice is flowing on a low permeable soft bed called till (in yellow). Chaotic crevassing is observed at the surface of the margins [*Harrison et al.*, 1998; *Echelmeyer and Harrison*, 1999]. Given the evidence we develop for internal melting, we hypothesize that a channelized drainage (in blue) exists at the margins along the bed and collects the water produced within the ice sheet above. The channel's diameter grows with distance downstream.

2. Model of partially melted margins: thickness of temperate ice

Siple Coast Ice Stream (SCIS) margins are subjected to internal heat production from straining, especially from lateral shear deformation of the ice. We first incorporate the ice deformation-heating work in a standard 1-D vertical heat transfer analysis and find evidence of internal melting at the margins. We thus write a 1-D model with a full temperature dependence of ice properties allowing for a temperate zone when the shear strain rate is sufficient. We find that all SCIS margins are at or very close to a strain rate level sufficient to partially melt the ice sheet. Hence we argue that internal melting within the ice sheet is in fact related to why margins are where they are. Finally, we use a detailed strain rate profile determined at the Dragon margin of Whillans ice stream B2 (Whillans IS B2) to characterize the transverse (perpendicular to the downslope direction) melting profile.

2.1. Evidence of internal melting at SCIS margins

Let us consider an ice stream cross section as depicted in figure 1. The ice stream is flowing in the downstream direction x, y is transverse to the flow and positive outward from the stream center and z is the vertical coordinate taken positive upward from the base of the ice (the notations used in this paper are reported in the Notation section). Let (u, v, w) be the velocity components associated to the (x, y, z) coordinates. Let us define respectively the lateral shear stress on lateral planes through the ice sheet oriented parallel to the flow and the basal shear stress as $\tau_{lat} = -\tau_{xy}$ (where $y > 0$) and $\tau_{base} = -\tau_{xz}$. This ice stream is driven by a gravitational driving stress, force per unit base area, $\tau_{grav} = \rho_{ice} g H S$ where ρ_{ice} is the ice density, g the acceleration due to gravity, H is the ice sheet thickness and S the absolute value of the surface slope that measures the inclination of the slab. A simple force balance at a distance y from the center of an ice stream, that considers a laterally constant thickness H, and neglects any variation in net axial force in the sheet [*Whillans and Van Der Veen*, 1993], shows that the thickness-averaged $\tau_{lat} = \tau_{lat}(y)$ increases with distance y from the center, scaling with an average over the distance y of the difference between the gravitational stress and basal resistive stress:

$$\tau_{lat}(y) H = (\tau_{grav} - \tau_{base})_{avg}\, y \qquad (1)$$

The lateral strain rate transverse to the downslope direction and predicted by Glen's law ($\dot{\gamma}_{lat} = 2A\tau_{lat}^3$ where the "engineering" shear strain rate is $\dot{\gamma}_{lat} = -2\dot{\epsilon}_{xy}$ where $y > 0$) increases as τ_{lat}^3. Then, the heating work rate $\tau_{lat}\dot{\gamma}_{lat}$ associated with the lateral deformation of ice increases as τ_{lat}^4 hence roughly proportionally to y^4. It quickly becomes a significant heat source within the ice sheet with increasing width, and must ultimately induce internal melting at

a large enough distance from the center of the stream, if some process does not limit stream expansion. That is why we later introduce the shear heating in a thermal model of well-developed margins.

The heat transfer equation, assuming a volumetric rate of internal heat production Φ, from deformation-heating within an ice sheet, is

$$\Phi - \vec{\nabla} \cdot \vec{q} = \rho_{ice} C_i \left(\frac{\partial T}{\partial t} + \left(\vec{v} \cdot \vec{\nabla} \right) T \right) \quad (2)$$

where $\vec{q}$ refers to the ice heat flux vector, ρ_{ice} the ice density, C_i the ice specific heat, t the time, $\vec{v}$ the ice velocity vector and T the ice temperature. Using Fourier's law, $\vec{\nabla} \cdot \vec{q} = \vec{\nabla} \cdot (-K \vec{\nabla} T)$ where K is the thermal conductivity. Rewriting in a 1-D approximation, $T = T(z,t)$, the previous equation now gives the equation governing the vertical temperature distribution of an ice column and it reduces at steady state, $T = T(z)$, to

$$\frac{\mathrm{d}}{\mathrm{d}z} \left(K \frac{\mathrm{d}T}{\mathrm{d}z} \right) - \rho_{ice} C_i w \frac{\mathrm{d}T}{\mathrm{d}z} + \Phi = 0 \quad (3)$$

where w is the vertical (z direction) component of $\vec{v}$. Since there are only a few measured temperature profiles with depth (especially at shear margins where access conditions are dangereous [*Harrison et al.*, 1998]), this latter 1-D thermal model is often used with a constant thermal conductivity, a simple vertical velocity profile and no shear heating (that is to neglect vertical shear within the ice column and lateral shear at the margins) because it allows a simple analytical solution (e.g., *Joughin et al.* [2002] used it to find a depth-average creep parameter and *Joughin et al.* [2003] to find the basal temperature gradient under Ross ice streams). We later suggest an analytical solution that incorporates the deformation-heating work rate.

This most commonly used analytical steady state solution (*Zotikov* [1986], relation 4.17) solves the equation

$$\alpha_{th} \frac{\mathrm{d}^2 T}{\mathrm{d}z^2} + \frac{az}{H} \frac{\mathrm{d}T}{\mathrm{d}z} = 0 \quad (4)$$

of vertical heat diffusion-advection neglecting any deformation-heating work rate Φ and taking K and $\rho_{ice} C_i$ as constant, for a bed temperature at the pressure-melting point T_{melt} and atmospheric temperature T_{atm} at the surface. For that, the thermal diffusivity, $\alpha_{th} = K / \rho_{ice} C_i$, is a constant and a is the "surface accumulation rate" in m.yr^{-1}. Also, a linear vertical velocity profile $w(z) = -az/H$ is assumed that cools the ice column via the motion of cold ice from the top, and any basal melting rate or freeze-on rate is neglected, i.e., $v_m \equiv -w(z=0) = 0$. In fact, this linear velocity profile comes from

$$w(z) = -v_m - \int_0^z \left[\frac{\partial u}{\partial x} + \frac{\partial v}{\partial y} \right] \mathrm{d}z \quad (5)$$

in which the downslope stretching $\partial u / \partial x$ is roughly estimated as a/H and any transverse velocity gradient is neglected to give the relation

$$w(z) = -v_m - \frac{az}{H} \quad (6)$$

However, at shear margins this *Zotikov* [1986] 1-D thermal model suffers from several issues: (1) Lateral deformation of ice induces a significant work rate, $\Phi = \tau_{lat} \dot{\gamma}_{lat}$ (neglecting the heating from other stress components). (2) The transverse velocity gradient $\partial v / \partial y$ may need to be considered, in that the margin temperatures are sensitive to the influx of colder ice from the slow ridge zone [*Jacobson and Raymond*, 1998]. Given the limited study (e.g., *Echelmeyer and Harrison* [1999]), we choose to neglect those transverse gradients in what follows and discuss their possible thermal effect later (cf. Discussion section). (3) Basal vertical velocity $-v_m$ may vary rapidly as we move toward the ridge and is poorly constrained.

We thus intend to find a more accurate 1-D thermal model of a column of ice at margins. This column is subject to shear heating, an atmospheric temperature at the top and a melting temperature at its base since water is present at ice-till interface [*Vogel*, 2004; *Vogel et al.*, 2005]. We incorporate the shear heating in a 1-D vertical heat transfer analysis that considers diffusion and advection as written in

$$\alpha_{th} \frac{\mathrm{d}^2 T}{\mathrm{d}z^2} + \left(\frac{az}{H} + v_m \right) \frac{\mathrm{d}T}{\mathrm{d}z} + \frac{\tau_{lat} \dot{\gamma}_{lat}}{\rho_{ice} C_i} = 0 \quad (7)$$

taking the thermal conductivity K and the specific heat capacity C_i as a constant (a restriction that is lifted in the

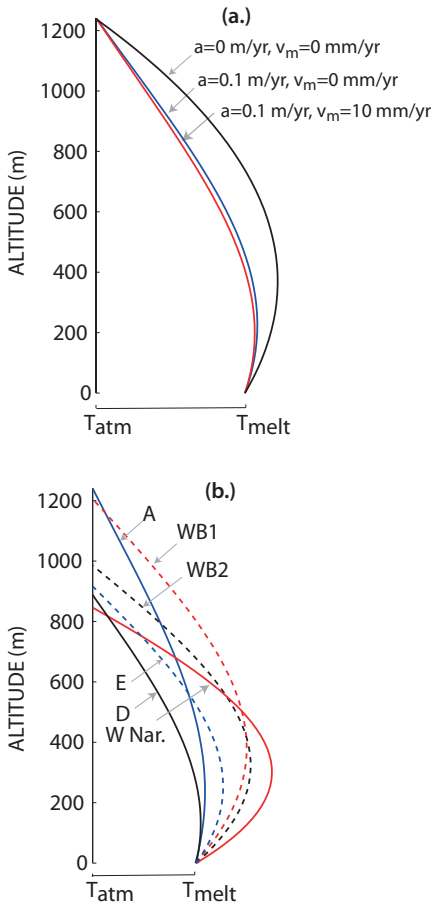

Figure 2. Temperature solution of the 1-D diffusion-advection model with shear heating as an internal heat source written in equation (7), a thermal diffusivity α_{th} of 1.3×10^{-6} m^2.s^{-1} and an atmospheric temperature T_{atm} of -26 °C. (a.) Ice sheet thickness, strain rate and melting temperature are taken from margin of Mercer ice stream (Table 1). Basal temperature gradient is positive for the three advection profiles used. (b.) Temperature profiles at margins of Mercer (A), Whilans (WB1, WB2 and W Nar.), Bindschadler (D) and MacAyeal (E) with $a = 0.1$ m.yr^{-1}, $v_m = 0$ m.yr^{-1} and parameters reported in Table 1. The basal temperature gradient is positive for the 6 profiles and thus $T > T_{melt}$ is (unrealistically) predicted, implying that a zone of temperate ice must exist.

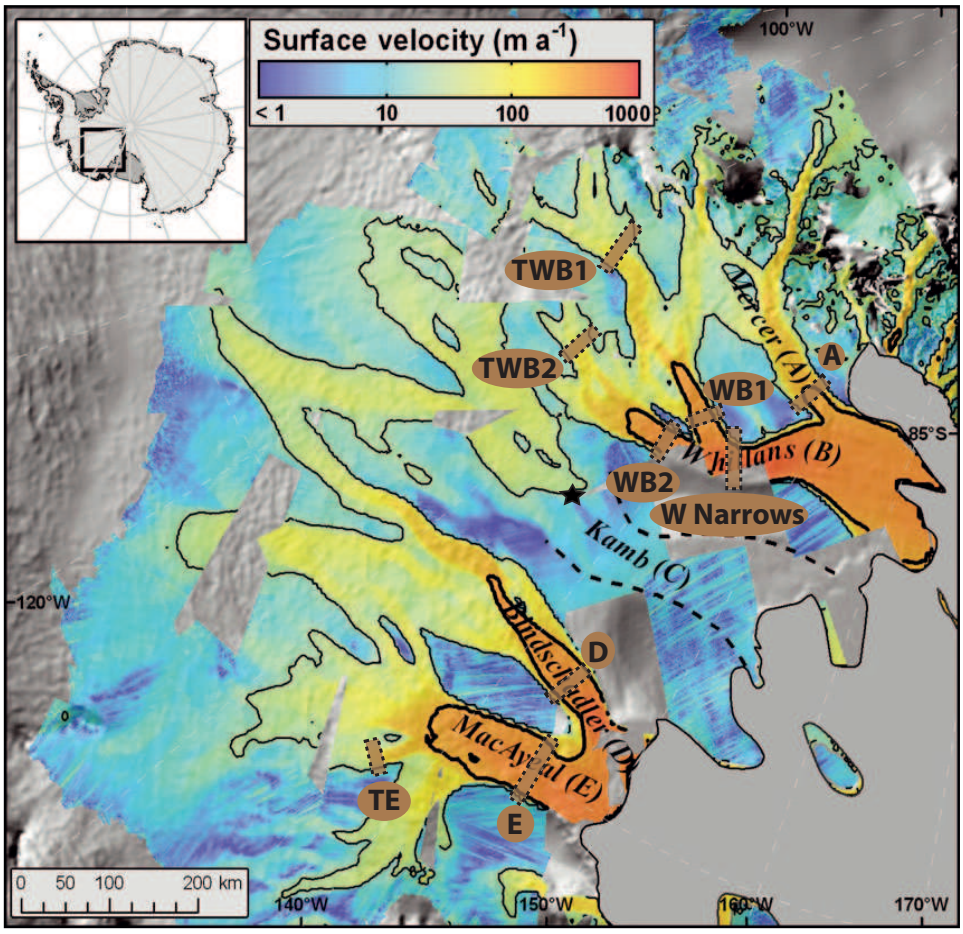

Figure 3. Surface velocity of Siple Coast ice streams, modified from *Brocq et al.* [2009]. Velocity contours shown are 25 m.yr^{-1} (thin line) and 250 m.yr^{-1} (thick line). *Joughin et al.* [2002] made profiles represented by brown lines and named in the brown circles or ovals to extract the parameters reported in Table 1. Profile TE, TWB1 and TWB2 are respectively made at tributary of MacAyeal, Whillans B1 and Whillans B2 ice stream before onset of streaming flow. The black star indicates the location of a borehole made at one shear margin of Kamb ice stream by *Vogel et al.* [2005]. They penetrated a 1.6 m tall liquid-filled cavity between the bottom of the ice and the bed. Using the JPL Ice Borehole Camera, they observed horizontal acceleration of small solid particles sinking into it, indicating a still active flow of water within the cavity (the direction of flow was not reported).

next subsection). To make a rough estimate in this section of the temperature profile, we evaluate the thermal diffusivity α_{th} and the specific heat capacity C_i at T_{avg} where $T_{avg} = (T_{atm} + T_{melt})/2$.

We adopt here a simple model based on the approximation, like in *Echelmeyer et al.* [1994] and *Scambos et al.* [1994], that the lateral shear strain rate is uniform over depth (which of course becomes questionable where the sheet is frozen to the bed). Thus the lateral shear stress is estimated, using Glen's law, as $\tau_{lat} = A(T)^{-1/3}(\dot{\gamma}_{lat}/2)^{1/3}$ where T, and hence τ_{lat}, varies with depth.

First, in this subsection, because it allows a simple analytical solution, we treat τ_{lat} as constant over depth, as

$$\tau_{lat} = A_{avg}^{-1/3}(\dot{\gamma}_{lat}/2)^{1/3} \tag{8}$$

with $A_{avg} \equiv A(T_{avg})$. Using $T_{atm} = -26$ °C, $a = 0.1$ m.yr^{-1} [*Joughin et al.*, 2003], $A_{avg}^{-1/3} \sim 521$ kPa.yr$^{1/3}$ [*Cuffey and Paterson*, 2010], and ice thickness and shear strain rate as measured at Mercer ice stream margin and reported in Table 1, we find that, because of the shear heating, we predict temperatures in excess of the melting temperature over a substantial fraction of the ice sheet thickness (Figure 2a). If the linear vertical velocity profile is valid at margins, numerical solutions show that the downward motion of cold ice at a rate of $a = 0.1$ m.yr^{-1} at the top cools the ice column whereas the basal melting rate $v_m > 0$ at the base does not significantly change the temperature profile and hence could be neglected in equation (7). Thus, for $v_m = 0$, the analytical solution of equation (7) which matches the boundary conditions $T(z = 0) = T_{melt}$ and $T(z = H) = T_{atm}$ is

$$\begin{aligned} T(z) &= T_{melt} + \sqrt{\frac{\pi}{2P}} H G_0 \,\mathrm{erf}\left(\sqrt{P/2}\,(z/H)\right) \\ &\quad + \frac{\tau_{lat}\dot{\gamma}_{lat}H^2}{K_{avg}P}\int_0^1 \frac{1-\exp\left(-\lambda P z^2/2H^2\right)}{2\lambda\sqrt{1-\lambda}}\,\mathrm{d}\lambda \end{aligned} \tag{9}$$

with G_0 being the temperature gradient $(\mathrm{d}T/\mathrm{d}z)_{z=0}$ at the ice-till interface,

$$\begin{aligned} G_0 &= \frac{2\sqrt{P/2}}{\sqrt{\pi}H\,\mathrm{erf}\left(\sqrt{P/2}\right)}\left(T_{atm} - T_{melt}\right. \\ &\quad \left. - \frac{\tau_{lat}\dot{\gamma}_{lat}H^2}{K_{avg}P}\int_0^1 \frac{1-\exp\left(-\lambda P z^2/2H^2\right)}{2\lambda\sqrt{1-\lambda}}\,\mathrm{d}\lambda\right) \end{aligned} \tag{10}$$

Table 1. Parameters used for margins of the profiles located in Figure 3. TWB1, TWB2 and TE are profiles made at, respectively, the tributaries of Whillans B1, Whillans B2 and MacAyeal ice stream.

Ice Stream	Profile	H[a] (m)	W[b] (km)	T_{melt}[c] (° C)	$\dot{\gamma}_{lat}$[d] (10^{-2}.yr^{-1})	A_{melt}[e] (10^{-24} s^{-1}.Pa^{-3})	B_{melt}[e] (kPa.yr$^{1/3}$)
Mercer	A	1242	39	−0.8	4.2	2.11	247
Whillans	WB1	1205	35	−0.8	7.0	2.11	247
	WB2	985	34	−0.6	9.5	2.19	244
	W Narrows	846	48	−0.6	13.5	2.19	244
	TWB1	2188	25	−1.5	3.8	1.85	258
	TWB2	1538	25	−0.9	4.0	2.07	249
Bindschadler	D	888	55	−0.6	5.8	2.19	244
MacAyeal	E	916	78	−0.6	8.1	2.19	244
	TE	1177	19	−0.8	5.5	2.11	247

[a] Ice sheet thickness as measured by *Joughin et al.* [2002].

[b] Ice stream width inferred by *Joughin et al.* [2002].

[c] Melting temperature at bed. When allowing for a temperate zone in modeling, we set this temperature to be the uniform melting temperature over depth.

[d] Shear strain rate $\dot{\gamma}_{lat}$ measured by *Joughin et al.* [2002]. These data suppose that the strain rate is symmetric relative to the ice stream center, i.e., $\dot{\gamma}_{lat}$ is of equal magnitude at both margins of the stream considered.

[e] Creep parameter at the basal melting temperature; see Appendix B for details on A and B as a function of temperature.

where the Péclet number $P \equiv Pe = aH/\alpha_{th}$ (cf. appendix A). When we neglect the shear heating product $\tau_{lat}\dot{\gamma}_{lat}$, this reduces to the solution of equation (4) already found by *Zotikov* [1986],

$$T(z) = T_{melt} + (T_{atm} - T_{melt}) \frac{\mathrm{erf}\left(\sqrt{P/2}\,(z/H)\right)}{\mathrm{erf}\left(\sqrt{P/2}\right)} \quad (11)$$

For a set of 6 active ice stream profiles (A, WB1, WB2, W Narrows, D, E) running across respectively Mercer, Whillans, Bindschadler and MacAyeal ice stream (see Figure 3), the lower part of the temperature profile at the margins predicted by relation (9) shows temperature in excess of melting (cf. Figure 2b) i.e., $G_0 > 0$ using parameters as reported in Table 1. Ultimately we presume that the ice sheet is temperate over some depth range hence supporting the possibility that internal melting within the ice sheet is indeed related to why the active margins are where they are.

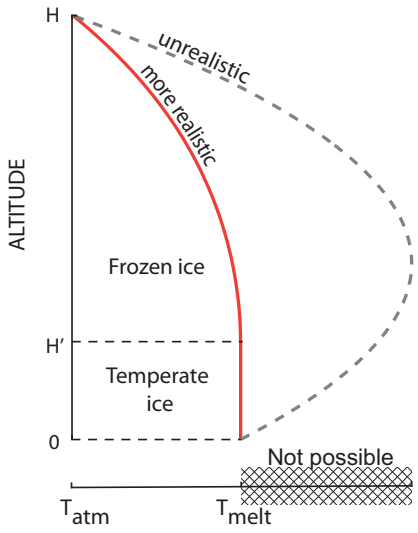

Figure 4. Sketch of the 1-D thermal model of a partially melted margin of Siple Coast ice streams. A height H' is at the melting point taken to be the pressure-melting point at bed and uniform over depth, so that there is no vertical heat conduction in this lower layer. The temperature in the rest of the ice sheet (frozen ice upper part) is predicted by a 1-D diffusion-advection heat transfer analysis with internal heating due to ice deformation.

2.2. Model set up, allowing for temperate zone and full temperature dependence of ice properties

Since the ice temperature could not be greater than T_{melt} as the previous simplified model predicted, we next solved a 1-D diffusion-advection heat transfer analysis allowing local internal melting and a temperature capped at the melting point such that a height H' of ice, adjoining the bed, is temperate (see Figure 4). The lateral shear strain rate, $\dot{\gamma}_{lat}$, is again taken uniform through the ice thickness. τ_{lat} is now the local shear stress on lateral planes through ice sheet oriented parallel to the flow. It is directly related to the temperature profile via the creep law since the creep parameter A is temperature dependent. Consequently the local volumetric rate of internal heat production is

$$\tau_{lat}(T)\dot{\gamma}_{lat} = 2A(T)^{-1/3}\left(\frac{\dot{\gamma}_{lat}}{2}\right)^{4/3} \quad (12)$$

The temperature dependence of the creep parameter is treated explicitly using the function proposed by *Cuffey and Paterson* [2010] (page 72) which fits results from field analyses and laboratory experiments; see the Appendix B. Thermal conductivity K and specific heat C_i of ice are also allowed to vary with respect to temperature T. Following the discussion on the forms of the dependence of these two latter parameters on T, in Kelvin (K), by *Cuffey and Paterson* [2010] (page 400), we use

$$K(T) = 9.828\ \frac{\mathrm{W}}{\mathrm{m.K}}\ \exp(-5.7\times10^{-3}\ \frac{T}{\mathrm{K}}) \quad (13)$$

$$C_i = 152.5\ \frac{\mathrm{J}}{\mathrm{kg.K}} + 7.122\ \frac{T}{\mathrm{K}} \quad (14)$$

The governing equation of our more refined but still 1-D model is now

$$\frac{\mathrm{d}}{\mathrm{d}z}\left(K(T)\frac{\mathrm{d}T}{\mathrm{d}z}\right) + \rho_{ice}C_i(T)\frac{az}{H}\frac{\mathrm{d}T}{\mathrm{d}z} + 2A(T)^{-1/3}\left(\frac{\dot{\gamma}_{lat}}{2}\right)^{4/3} = 0 \quad (15)$$

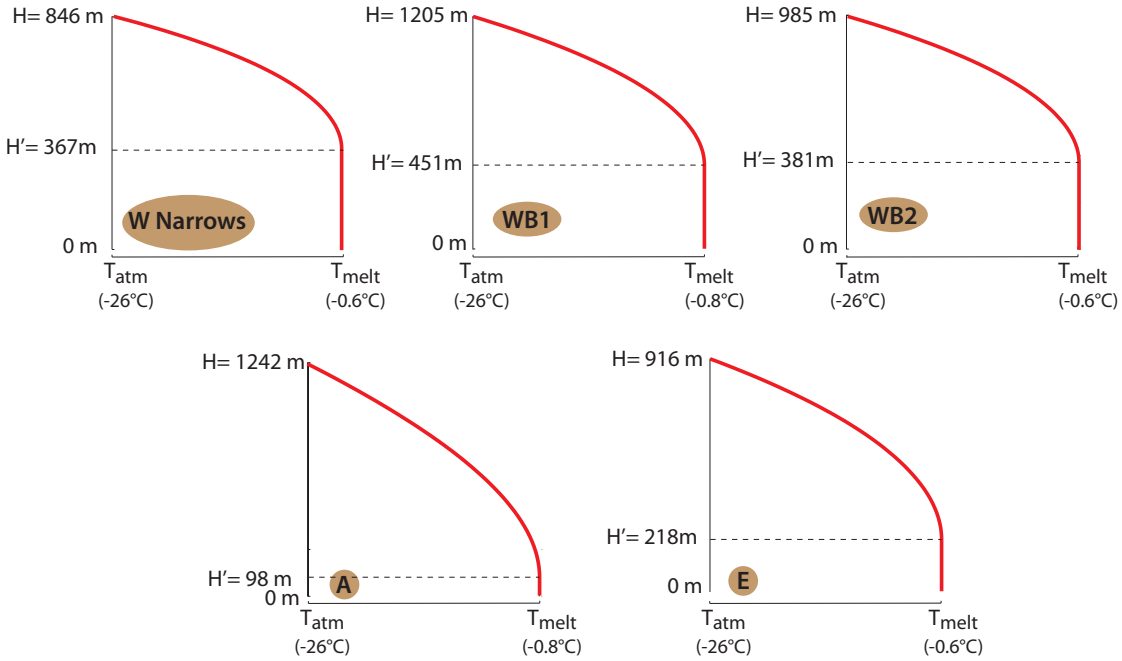

Figure 5. Temperature profile predicted by the 1-D thermal model of margins of profiles located in Figure 3 for an ice sheet thickness and a lateral strain rate as reported in Table 1. Where margins have been sampled by *Joughin et al.* [2002], respectively 8, 43 and 24 % of the ice height of the Mercer, Whillans and MacAyeal ice streams is temperate. The model predicts, for the strain rate and thickness given, that respectively 37 and 39 % of the ice height of tributary B1 and B2 of Whillans ice stream is temperate. The strain rate level measured at Bindschadler ice stream (0.058 yr^{-1}) is not enough to melt a portion of the 888 m ice thickness, although onset of melting i.e., $H' = 0^+$, would be predicted for a 5 % increase to 0.061 yr^{-1}. Also, as one moves $\sim$ 30 km downstream the maximum strain rate observed at the Bindschadler stream south margin increases far in excess of that, by $\sim$ 280 % and reaches 0.16 yr^{-1} [*Scambos et al.*, 1994]. For a comparable ice thickness of what has been measured at profile D, that level of strain rate would melt 53 % of the ice sheet thickness according to our model.

T in the upper part of the ice sheet, where the ice is frozen, and H', the height of temperate ice adjoining the bed, are the unknowns (cf. Figure 4). Mathematically, this takes the form of a free boundary problem in 1-D. The equation is solved subject to boundary conditions $T(z = H) = T_{atm}$, $T(z = H') = T_{melt}$ and dT/dz=0 at $z = H'$. Indeed we set T_{melt} at its temperature for a pressure equal to the overburden pressure at the bed, a function of the ice thickness of the stream considered (cf. Table 1). We do not further take into account the pressure dependence of the melting point i.e., T_{melt} does not depend on z. Consistently with this assumption, we solve equation (15) with a temperature gradient equal to zero at $z = H'$.

When the level of strain rate is enough to melt the ice sheet, we allow some lower depth range to be partially melted at $T = T_{melt}$ and the rest of the temperature profile is predicted by equation (15). Therefore, the solution of this model, found numerically by standard Runge-Kutta procedures and shooting techniques, gives the proportion of the ice sheet that is temperate depending on the ice sheet thickness and the shear strain rate imposed. For all the ice streams we set $T_{atm} = -26\,^{\circ}C$ and the surface accumulation rate a at 0.1 $m.yr^{-1}$ [*Joughin et al.*, 2003].

2.3. What fraction of the ice thickness is temperate at the margins ?

Nine ice stream transverse (across the flow) downslope velocity profiles have been made by *Joughin et al.* [2002]; see Figure 3. We use their measurements of strain rate and ice thickness of active SCIS margins, reported in Table 1, for our thermal regime modeling. These lateral strain rate measurements inferred from downstream velocity profiles are somehow decreased by the 3.5 km smoothing filter used to reduce the noise. Indeed they could not recognize a jump in strain rate that occurs, for example, over a distance of less than 2 km at a margin of Whillans ice stream B2 (see the shear strain rate profile made at the south margin of Whillans IS B2 reported in Figure 7a) so that we might expect actual values of strain rate peaks at margins higher than the ones displayed in Table 1. Besides, *Scambos et al.* [1994] have made a series of ice-speed profiles and found that the maximum ice speed and strain rate at the south margin of Bindschadler ice stream increase dramatically from 420 to 670 $m.yr^{-1}$ and 0.02 to 0.16 yr^{-1} as the margin develops along only 55 km in the downstream direction. Consequently the results presented in that section and predicted by our 1-D model of temperate margins are valid for the particular downstream location considered i.e., for the specific ice sheet thickness and strain rate value reported in Table 1.

Our analysis predicts that almost all active ice streams where sampled are at a level of strain rate at which internal melting occurs (cf. Figure 5). Respectively 8, 37, 39, 43 and 24 % of the ice thickness of Mercer, Whillans B1, Whillans B2, Whillans and MacAyeal ice stream margins are predicted to be temperate (see ratio H'/H in Table 2). The strain rate level measured at Bindschadler ice stream (0.058 yr^{-1} at margins of profile D) is not enough to melt a portion of the 888 m ice thickness, although onset of melting i.e., $H'/H = 0^+$, would be predicted for a 5 % increase to 0.061 yr^{-1}. Also, as one moves $\sim$ 30 km downstream the maximum strain rate observed at the Bindschadler stream south margin increases far in excess of that, by $\sim$ 280 % and reaches 0.16 yr^{-1} [*Scambos et al.*, 1994], as noted. For

Table 2. Ice streams gravitational driving stress as measured at profiles located in Figure 3 and calculated temperate fraction, lateral stress, basal shear stress and ratio of basal stress to driving stress, neglecting the gradient in net axial force.

Ice Stream	Profile	τ_{grav}[a](kPa)	H'/H [b](%)	$\bar{\tau}_{lat}$ (kPa)	τ_{base} (kPa)	τ_{base}/τ_{grav} (%)
Mercer	A	14.9	8	119.0	7.7	52
Whillans	WB1	12.5	37	115.6	4.5	36
	WB2	10.8	39	127.0	3.4	32
	W Narrows	7.6	43	138.5	2.7	36
Bindschadler	D	10.0	0[c]	131.7	5.7	58
MacAyeal	E	15.3	24	128.9	12.3	80

[a] Inferred by *Joughin et al.* [2002],$\tau_{grav} = \rho_{ice} g H S$ where S is the downstream slope.

[b] Predicted temperate height fraction of the ice sheet at margin.

[c] The ratio increases to $\sim$ 53 % when evaluated 30 km downstream (see text).

a comparable ice thickness to what has been measured at profile D, that level of strain rate would melt 53 % of the ice sheet thickness according to our model.

Our studies also predict, for the strain rate and thickness given by *Joughin et al.* [2002], that some margins of tributaries of Siple Coast ice streams are also in a state of partial melt, with temperate ice being present over a fraction of the ice sheet adjoining the bed. The fractions of the marginal ice sheet thickness of profiles E, TWB1 and TWB2, respectively made at tributary of MacAyeal, Whillans B1 and Whilllans B2 (cf. Figure 3) that are predicted to be temperate is respectively 23, 26 and 50 % (see ratio H'/H in table 3). However profiles made farther upstream than profile D at Bindschadler ice stream and profiles made at the active upper part of Kamb ice stream are not predicted to have marginal temperate ice. At that active upper part of Kamb ice stream, the ice flow does not have the characteristics of streaming flow (e.g., almost twice the thickness of other streams and a low marginal strain rate, less than 0.01 yr^{-1}).

We also explore the results given by the model when the vertical advection of ice is absent i.e., when the downslope stretching matches the transverse compression of ice at margins, which may occur as a consequence of ice mass lost through the melting process (a concept developed later). In this case we found that respectively 22, 42, 42, 46, 11 and 32 % of the ice height of Mercer, Whillans B1, Whillans B2, Whillans, Bindschadler and MacAyeal ice stream margins is temperate. The motion of cold ice from the top of the column diminishes the predicted height of temperate ice, as expected.

2.4. Ice stream force partitioning that considers temperate ice at margins

Since we emphasize having a more accurate temperature profile at margins, we evaluate the side drag in order to quantify the force partitioning i.e., how much of the gravitational driving stress is balanced by basal shear stress and lateral drag assuming insignificant gradient in axial force.

Let us define the creep parameter $B = A^{-1/3}$, so that $\tau = B(T)(\dot{\gamma}/2)^{1/3}$, with B_{melt} being its value at the melting point and B_{fl} the depth-averaged value of the temperature-dependent creep parameter B in the frozen layer of the ice sheet; see Appendix B for a detailed description of the temperature dependency of this creep parameter. Thus, B_{melt} is the creep parameter we use in the lower part of thickness H' that is temperate (reported for each profile in Table 1) and B_{fl} the one use for the upper frozen layer of the profile over a height of $H - H'$.

$$B_{fl} = \frac{1}{H - H'} \int_{H'}^{H} B\left[T(z)\right] \mathrm{d}z \tag{16}$$

The average lateral shear stress $\bar{\tau}_{lat}$ over the ice sheet thickness, neglecting any porosity effect on strength in the temperate region, is calculated for each profile with the equation

$$\bar{\tau}_{lat} = B_{melt} \left(\frac{\dot{\gamma}_{lat}}{2}\right)^{1/3} \frac{H'}{H} + B_{fl} \left(\frac{\dot{\gamma}_{lat}}{2}\right)^{1/3} \frac{(H - H')}{H} \tag{17}$$

and reported in Table 2. Because we allow a height H', adjoining the bed, to be temperate, $\bar{\tau}_{lat}$ predicted by equation (17) is lower than the lateral shear stress estimated by *Joughin et al.* [2002] for frozen margins of similar thickness.

A simplified force balance of an ice stream that neglects any variation in net axial force in the sheet (shown to be accurate for Whillans ice stream [*Whillans and Van Der Veen*, 1993]) and transverse variation of ice thickness gives us the average basal shear stress τ_{base} over the width for each profile studied,

$$\tau_{base} = \tau_{grav} - \frac{2\bar{\tau}_{lat} H}{W} \tag{18}$$

Here W is the ice stream width, which is taken to be the distance between the two peaks in the transverse profile of lateral shear strain rate made by *Joughin et al.* [2002]. Using this latter relation and their values of ice thickness and stream width, we thus find higher values of basal drag. Still, these values, of order of 3 to 12 kPa, are clearly indicative of a weak bed underlying Siple Coast ice streams (cf. Table 2).

On Whillans ice stream B1 and B2 τ_{base} is estimated at 4.5 and 3.4 kPa. These values are higher than in-situ shear strength measurement of basal till (*Kamb* [2001] found a strength of 2 kPa near Up B, cf. Figure 6) and the range of 1.2 to 2.8 kPa found by *Joughin et al.* [2003] who used control method inversion of a high-resolution velocity data set to find the basal shear stress corresponding to a plastic bed. However, when they do consider an enhancement factor (E=3) that models the margins weakening due to shear heating their values are slightly larger than ours (5.8 and 5.3 kPa for B1 and B2). Consequently, even with a model that allows a height of the ice at margins to be temperate and ultimately treats the margin weakening expected there, the till under Whillans ice stream is inferred to be very weak. Additionally, we find that where Whillans stream is about 35 to 50 km wide (before the ice plain and at the two tributaries B1 and B2) the bed supports only around 35 % of the gravitational driving stress (Table 2). More measurements in the downstream direction from the tributaries to the ice plain could show if we recognize a special feature of this stream. Still, at tributaries of Whillans ice stream basal drag is moderate (about 30 kPa) and provides more resistance to the larger driving stress ($\sim$ 68 %, cf. Table 3).

On Mercer ice stream, the basal shear stress is about 7.7 kPa and supports 52 % of τ_{grav} (cf. table 2). We find that

Table 3. Tributaries gravitational driving stress as measured at profiles located in Figure 3 and calculated temperate fraction, lateral stress, basal shear stress and ratio of basal stress to driving stress, neglecting the gradient in net axial force.

Ice Stream	Profile	τ_{grav} [a](kPa)	H'/H [b](%)	$\bar{\tau}_{lat}$ (kPa)	τ_{base} (kPa)	τ_{base}/τ_{grav} (%)
Whillans	TWB1	47.5	50	90.8	31.6	67
	TWB2	40.9	26	101.9	28.4	69
MacAyeal	TE	44.9	23	113.6	30.8	69

[a] Inferred by *Joughin et al.* [2002], $\tau_{grav} = \rho_{ice} g H S$ where S is the downstream slope.

[b] Predicted temperate height fraction of the ice sheet at margin.

the basal drag is roughly 2.5 kPa stronger with a model that allows 53 m of the ice thickness to be temperate than with frozen ice at all depths [*Joughin et al.*, 2002].

Profile E of MacAyeal ice stream shows that this stream is wider than the other active ice streams (with the exception of the ice plain of Whillans ice stream) which seems to diminish the influence of lateral drag ($\tau_{base}/\tau_{grav} = 80\%$). The effect of temperate ice over 203 m at margin increases only by 1.5 kPa the predicted basal drag with frozen margins [*Joughin et al.*, 2002]. However, at MacAyeal ice stream much of the resistance is concentrated at a few sticky spots where τ_{base} reaches 50 kPa [*Fricker et al.*, 2010]. Nevertheless, our estimation of the average basal shear stress over the width of 12.3 kPa is coherent with control method inversions for a plastic bed over this region (14.9 kPa according to *Joughin et al.* [2003]).

These basal shear stresses are calculated as an average over the width. Small scale perturbations of τ_{base} occur as a result of the water pore pressure in the till, assuming that subglacial drainage is partly made of distributed flow and channelized drainage [*Schoof*, 2010; *Hewitt*, 2011]. Also, the numbers reported for τ_{base} are really to be thought of as a combination of the actual τ_{base} plus a poorly constrained contribution to overall force equilibrium from gradients in net axial force.

2.5. Detailed characterization of Dragon margin, Whillans ice stream B2

Dragon margin, an approximately 4 km wide marginal shear zone, is the south margin of Whillans ice stream B2, the limit between the stream and the ridge B1-B2 named Unicorn (Figure 6). The inter boundary of this margin is a $\sim$ 2 km wide region of large, but somewhat organized, crevasses whose density increases toward the margin. These crevasses roughly tend upstream at an angle of 40 ° to 70 ° to the margin, indicating an origin related to lateral shear τ_{lat}. This sub-zone ends rather abruptly at the chaotic zone. This last zone of $\sim$ 2 km width consists of highly disorganized crevasses and fractured ice blocks, a signature of elevated lateral shear stress. The outer boundary of Dragon margin, a sub-zone of $\sim$ 100 m width [*Echelmeyer et al.*, 1994], consists of large but widely spaced accurate crevasses. We do not represent this narrow sub-zone on Figure 6 or Figure 7. Profile S1, near to, but not the same as the WB2 profile, gives us a transverse profile of the downstream velocity. Over 5 km of distance the velocity decreases from 387 m.yr^{-1} at the north extremity of profile S1 to 2 m.yr^{-1} just outside of the margin i.e., south S1. In this domain the lateral shear strain rate varies from 0.01 to 0.15 yr^{-1}(Figure 7a). Between the middle of the stream and north of S1 the surface velocity observed does not change much; i.e., the lateral strain rate is close to zero. Since this profile gives us an excellent set of data to characterize the behaviour of a margin, we will use this profile in the rest of the paper.

Using our 1-D model we produce a profile of temperature versus height and show the fraction of the ice sheet near the margin which we predict to be temperate. We find that temperate ice at Dragon margin is predicted to reach a maximum 57 % of the ice sheet thickness and to be comparably high over slightly more than 2 km width at the bed (Figure 7a and Figure 8). Therefore, the width of temperate ice through the ice sheet approximately matches the width of the highly stressed chaotic crevassing zone that appears at surface.

We also explore the hypothesis that no vertical motion of ice occurs at the margin i.e., the downslope stretching matches the transverse compression of ice. We thus find that the predicted maximum height of the temperate region does not change whereas its width is slightly bigger (cf. Figure 8). Our analysis predicts that more than 10 % of the ice sheet thickness is temperate along a width of $\sim$ 3 km with vertical advection of ice and along $\sim$ 3.5 km without. We suggest that even if the vertical motion of ice is not yet well

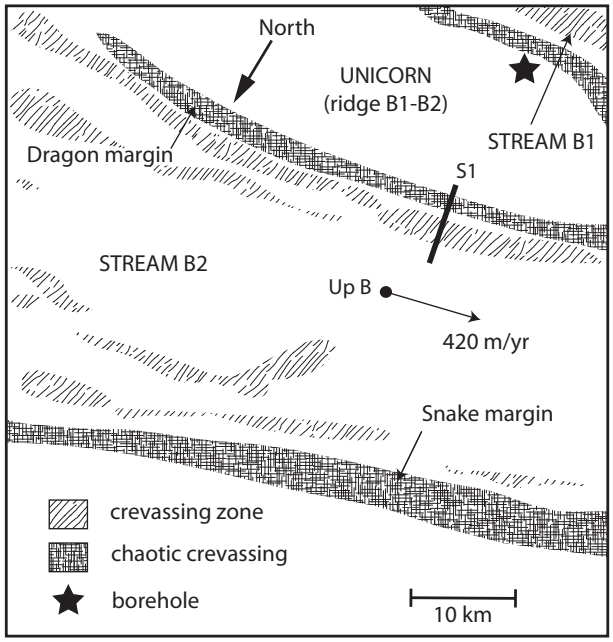

Figure 6. Location of profile S1 on Whillans ice stream B2 (see Figure 3) where *Echelmeyer et al.* [1994] measured a surface velocity profile to extract the Dragon margin shear strain rate profile. The black star at the interstream ridge between Whillans ice stream B1 and B2, an area commonly referred to as the Unicorn, indicates the location of a borehole made by a Caltech group (mentioned as a personal communication from H. Engelhardt by *Clarke et al.* [2000]). They encountered layers of high tip resistance to the drill at 56-49 m, 44-22 m, and 14-0 m above the bed. At UpB the ice velocity is measured at 420 m/yr. North-South axis is approximately perpendicular to Dragon margin. (redrawn and modified, based on *Echelmeyer and Harrison* [1999])

explained when neglecting the transverse motion of ice, the effect of the advection term does not make us reconsider the hypothesis of internal melting at margins.

3. Could melt onset control ice stream width ?

We have shown that shear heating induces a temperate zone at ice stream margins. The continuously deformation generates meltwater which gravity would cause to percolate toward the bed below. In this section we estimate the accumulated seepage rate along the Dragon margin's bed of Whilllans ice stream B2 based on our previous thermal modeling and the deformation data. Associated with seeping water along margin's bed a channelized marginal drainage of Röthlisberger type may develop, probably under the chaotic crevassing zone where the shear heating, and corresponding basal meltrate, is the highest. Standard theory argues that the high, nearly lithostatic, pore pressure elsewhere (i.e., near the bed within the fast moving stream) is somewhat alleviated within the channel, which operates at reduced water pressure [*Röthlisberger*, 1972; *Nye*, 1976]. That results in a higher Terzaghi effective normal stress acting along the bed just outside of the channel, and hence creates high resistance against frictional shear which plausibly locks the ice outboard of such channel to the bed, naturally forming an ice stream margin.

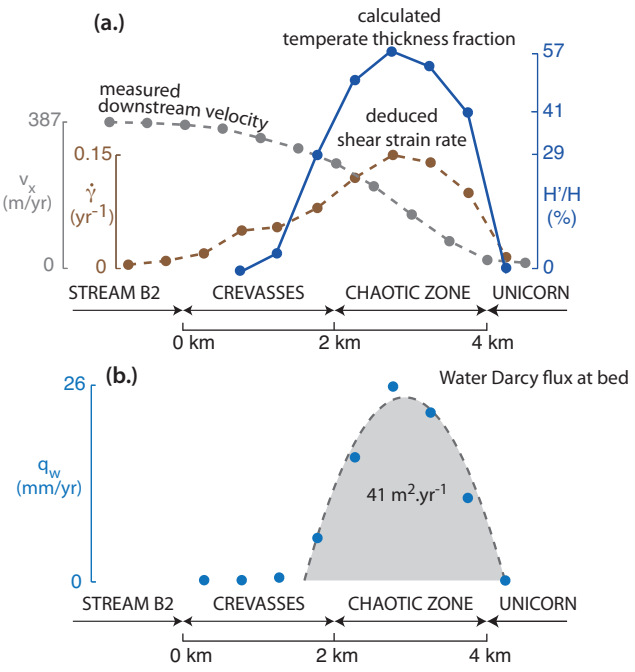

Figure 7. Detailed characterization of Dragon margin (profile S1 located on Figure 6). (a.) Measured downstream velocity (grey circles) gives the lateral shear strain rate profile (orange circles) [*Echelmeyer et al.*, 1994]. This later is inserted into our 1-D thermal model of a partially melted margin, which considers a constant ice sheet thickness $H = 985$ m, to estimate the temperate fraction H'/H and melting profile (in blue). Where the lateral strain rate is the highest (0.15 yr^{-1}) in the chaotic crevassing zone, 57 % of the ice sheet thickness is temperate. The downstream velocity is about 160 $\mathrm{m.yr}^{-1}$ and may also be associated with downslope stretching. Vertical motion (advection) of ice may thus occur, with assumed accumulation in order to keep the thickness at steady state, and our approximate advection profile may be still valid there. (b.) Darcy water flux at base of temperate ice calculated with equation (23) (blue circles). We predict that the shear heating could melt the near-bed ice over a 2 km width under the chaotic crevassing zone, producing a water flux, integrated across the base of the margin, of about 41 $\mathrm{m}^2.\mathrm{yr}^{-1}$ (second-order polynomial fit).

3.1. Drainage to the bed associated with melting causes Röthlisberger channel development

Within the temperate ice column of height H', water permeation occurs. Shear heating generates melt at a rate per unit of volume $\dot{m}$. Thus,

$$\dot{m} = \frac{\tau_{lat}\dot{\gamma}_{lat}}{L} \tag{19}$$

where $L = 335$ $\mathrm{kJ.kg}^{-1}$ is the latent heat per unit mass. Water in polycrystalline ice at its melting point forms a system of veins at three-grain junctions [*Nye*, 1989]. This water, both in veins and in other locations, may affect the creep rate of temperate ice by a factor $F(n)$, a function of n, the volume of internal meltwater per unit of volume of ice. Then the creep strength in temperate ice within the height H' is

$$\tau_{lat} = B_{melt}\left(\frac{\dot{\gamma}_{lat}}{2}\right)^{1/3} F(n) \tag{20}$$

and the melt rate per unit of volume becomes

$$\dot{m} = \frac{2B_{melt}}{L}\left(\frac{\dot{\gamma}_{lat}}{2}\right)^{4/3} F(n) \tag{21}$$

Meltwater, being more dense than its chemically identical solid phase (neglecting any contamination from above), seeps downward. Considering only vertical Darcy flux q_w of water, mass conservation $\nabla \cdot (\rho_w q_w) = -\dot{m}$ leads to

$$\frac{\mathrm{d}q_w}{\mathrm{d}z} = -\frac{2B_{melt}F(n)}{\rho_w L}\left(\frac{\dot{\gamma}_{lat}}{2}\right)^{4/3} \tag{22}$$

with $\rho_w = 1000$ $\mathrm{kg.m}^{-3}$ the density of water. This latter equation is integrated in z over the temperate ice thickness to find the flux at the bed, assuming again that the shear strain rate is uniform over depth and knowing that the Darcy

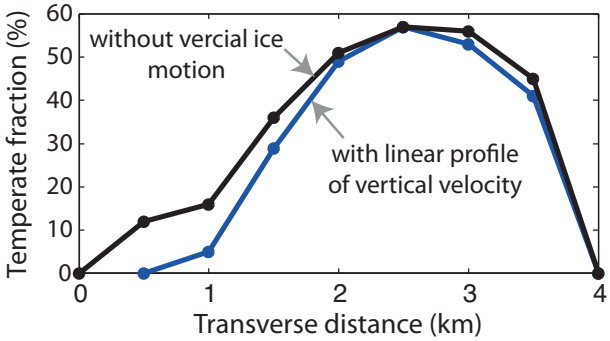

Figure 8. Fraction of the ice sheet thickness that is temperate at Dragon margin. The temperate region is narrower when the vertical advection is not taken into account in the 1-D model of partially melted margin. Nevertheless, the maximum temperate fraction of the height is predicted to be the same (57 %).

flux vanishes at the top of the temperate ice column. Thus,

$$(q_w)_{z=0} = \left[\frac{1}{H'}\int_0^{H'} F(n)dz\right] \frac{2B_{melt}H'}{\rho_w L}\left(\frac{\dot{\gamma}_{lat}}{2}\right)^{4/3} \quad (23)$$

A first approximation is to consider a small perturbation due to the porosity on the creep strength as $F(n) = 1 - cn^{\lambda}$ with $\lambda \geq 1$ and c a positive constant. As the water content per unit of volume of ice n is expected to be lower than 10^{-3} in a saturated veins system [*Nye and Frank*, 1973; *Jordan and Stark*, 2001] we hypothesize in this first treatment that the term in bracket is sensibly equal to unity. Therefore, the Darcy water flux at base of an ice column where internal melting occurs is only a function of the shear strain rate and the height of temperate ice which we predict with our previous thermal modeling allowing for a temperate zone. Using the transverse profile of observed strain rate and calculated temperate height of ice H' adjoining the bed made at the Dragon margin of Whillans ice stream B2 and depicted graphically in Figure 7a, the latter relation gives a transverse profile of basal meltwater rate (cf. Figure 7b). This deformation-induced seeping meltwater is localized only under the highly stressed chaotic crevassing zone where the maximum Darcy flux reaches 26 mm.yr^{-1}. That is an order of magnitude higher than the estimated basal meltwater rate due to basal friction inferred to be present at the center of this stream [*Joughin et al.*, 2003] and others Siple Coast ice streams [*Joughin et al.*, 2004b]. This model does not explicitly consider the reduced resistance to water flux due to basal crevasses [*Flowers and Clarke*, 2002], although ultimately it is the shear heating in the temperate zone that determines the net melting, and hence the water flux to the bed.

Vogel et al. [2005] drilled to the bottom of Kamb ice stream at the transition between the active upper part and its stopped main trunk (cf. Figure 3) and found that basal ice is devoid of air. We suppose that, at the base of the ice sheet, the veins are water saturated and the ice grains slide at their boundary allowing the water pressure to be equal to the ice overburden stress. This sliding allows the permeability to adjust to whatever value needed to transmit the meltwater generated, at least for a system operating in steady state. Along the bed the total downward flux of meltwater per unit area produced by shear heating may be expressed as in Darcy's law [*Lliboutry*, 1996],

$$q_w = -\frac{k_{ice}}{\mu_w}\left(\frac{\mathrm{d}p}{\mathrm{d}z} + \rho_w g\right) \quad (24)$$

where $\mu_w = 1.8\times10^{-3}$ N.s.m^{-2} refers to the dynamic viscosity of water and g the acceleration due to gravity. Because the water pressure in veins is equal to the ice overburden pressure $\mathrm{d}p/\mathrm{d}z = -\rho_{ice}g$. Thus, the temperate ice permeability, a function of the downward water Darcy flux, is

$$k_{ice} = \frac{q_w\,\mu_w}{(\rho_{ice} - \rho_w)\,g} \quad (25)$$

The Darcy flux estimated at the Dragon margin bed is about 26 mm.yr^{-1} (Figure 7b). We thus find a maximum ice permeability of 1.7×10^{-15} m^2, consistent with measurements of water saturated veins (*Jordan and Stark* [2001] found temperate ice permeability of 1 to 3×10^{-15} m^2).

We integrate the meltwater generated along the bed by shear heating over the $\sim$ 2 km width of the highly stressed chaotic crevassing zone of the Dragon margin where sampled (Figure 6). We find that 41 $m^3.yr^{-1}$ of meltwater emerge, along the ice-till interface, for each meter of length downstream (cf. Figure 7b).

We suggest that the relatively high water production found at the bed and localized in a narrow 2 km wide zone could cause a channelized marginal drainage development of Röthlisberger type (R-channel). We thus evaluate what would be the diameter of a R-channel, treated as having a semicircular cross section, if it collects from 100 km upstream a constant supply of 41 m^3.yr^{-1} of basal meltwater generated by shear heating for each meter of length downstream. The water discharge in m^3.yr^{-1} drained by this hypothetical R-channel would be Q_w =41 m^2.yr$^{-1}\times$ 100 km. Using the Manning formula for a turbulent flow in a pipe, in the particular form given by *Cuffey and Paterson* [2010], we write the discharge as a function of the hydraulic radius R_h

$$Q_w = \frac{A_c}{[\rho_w g]^{1/2}\, n_m} R_h^{2/3} G^{1/2} \quad (26)$$

where A_c refers to the cross-sectional area, $n_m \approx 0.1$ s.m$^{-1/3}$ is the Manning roughness coefficient, and G is the magnitude of the force per unit volume driving flow, roughly approximated by $G \approx \rho_w g S$. The downstream slope S of Whillans ice stream B2 measured near Up B (Figure 6) is 0.00123 [*Joughin et al.*, 2002]. Also, R_h, the hydraulic radius is, for the considered semicircular channel of diameter D,

$$R_h = \frac{D}{4(1 + 2/\pi)} \quad (27)$$

Thus, the diameter of this semicircular channel that drains a flux Q_w is

$$D = 2\left[\frac{4Q_w\,(\rho_w g)^{1/2}\, n_m\,(1 + 2/\pi)^{2/3}}{\pi G^{1/2}}\right]^{3/8} \quad (28)$$

As the channel is continually collecting basal meltwater generated by shear heating, its diameter grows in the downstream direction. The accumulated seepage along the bed at the estimated rate at Dragon margin where sampled by *Echelmeyer and Harrison* [1999] (41 m^3.yr^{-1} for each meter of length downstream), if prevailing over 100 km upstream, is consistent with a semicircular Röthlisberger channel of diameter $D = 1.5$ m. This simple estimation does neglect any migration of water toward the center of the stream due to the bed transverse slope of the ice surface near the margin (Joughin, personal communication).

3.2. Limit to the stream width by lockage to the bed outboard of channels

As predicted by standard theory of drainage system, a greater melt supply to a channel results in a higher discharge and, thus, a larger effective stress (lower water pressure). Using the fundamental equation of steady-state tunnel theory [*Röthlisberger*, 1972; *Nye*, 1976], we can write what would be the effective stress N_c (ice overburden pressure minus water pressure in the channel) along the ice-till interface just outboard of a channel as a function of the water discharge. That is [*Cuffey and Paterson*, 2010]:

$$N_c = K_2 \frac{G^{11/24} Q_w^{1/12}}{n_m^{1/4} A_{melt}^{1/3}} \quad (29)$$

with:

$$K_2 = \left[(\rho_i L_f K_1)^{1/3} (\rho_w g)^{1/8}\right]^{-1} \quad (30)$$

and $K_1 = [2/27]\,[4\pi]^{1/4} \approx 0.139$. If we again consider a channel that collects from 100 km upstream a constant water supply as generated at Dragon margin near Up B

(41 $m^3.yr^{-1}$ for each meter of downstream length, cf. Figure 7b), we find a Terzaghi effective stress acting along the bed just outboard of the channel of 179 kPa. This is nearly two orders of magnitude larger than the predicted effective stress at the center of the Whillans ice stream B2, where $N_s = \tau_{base}/f = 1.8$ kPa assuming a friction coefficient of $f = 0.5$ (cf. Table 2), and hence creates high resistance against frictional basal shear, firmly pressing the ice against the till bed.

Ice streams are underlain everywhere by a plastic bed [*Tulaczyk et al.*, 2000]. If the basal shear stress equals the yield strength of the bed everywhere under the stream then downslope sliding occurs while the ridges are locked, frozen to the bed. This anti-plane shear crack like feature (see Figure 9) induces stress singularities at the margins. High stress concentrations on the ice-stream side of the margin have been found either analytically when considering the ice as a Newtonian fluid with constant viscosity [*Schoof*, 2004] and numerically when ice rheology is treated with Glen's law [*Jacobson and Raymond*, 1998]. To prevent the shearing crack growth due to high stress concentration at the tip, we note that standard theory of fracture mechanics argues that a hole in a thin plate can stop a tensile crack that is growing in the plate. The crack can grow into a hole but not so easily propagate out because then the stress concentration at its tip is much reduced. We may think of the ice stream and bed as an analogous system, now containing an anti-plane crack whose surface is the base of the ice sheet beneath the stream and whose tip lies along the shear margin. We suggest that the easiest way to stop an outward propagation of such a crack, that is, to stop outward margin migration, is to alleviate the stress concentration at the crack tip. That would be accomplished by having the tip region be replaced by a long marginal channelized drainage such as we have suggested, leaving a situation analogous to a crack whose tip has propagated into a hole (cf. Figure 9).

The elevated Terzaghi clamping stress which we have estimated along the bed should occur on both the inboard and outboard sides of the channel. However, downstream slip at the bed would plausibly not be stopped on the inboard side of the marginal channelized drainage, because that would re-create a situation of a crack without a blunted tip which could, despite the elevated Terzaghi clamping stress, continue to propagate until it reaches the channel. Once having propagated into the channel, it would have greatly diminished stress concentration and hence would not induce basal slip on the outboard side of the channel, which would be under comparably high clamping stress.

We conjecture that this channelized development at ice stream margins locks the ice outboard to the bed, naturally creating a limit to the region of fast-flowing ice. It is beyond the scope of our paper to fully quantify such a process but it is consistent with ice streams existing at a width which corresponds to rapid internal melt generation as our results here have suggested (see Figure 5 and Table 2 and 3).

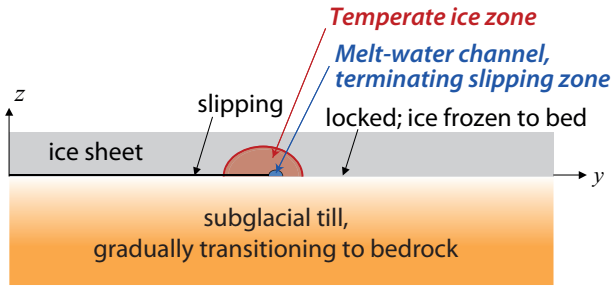

Figure 9. Conjectured stable configuration of an ice stream shear margin near the bed. The transition between slipping and locked zones at an ice sheet bed defines an anti-plane shear crack whose surface is the base of the ice sheet beneath the streaming flow (thick black line) and whose tip lies along the shear margin. Because cracks strongly concentrate stress and strain rate near their tips, the shear heating and hence the basal meltwater generation should be most intense in that near-tip region and might induce meltwater channel formation. Both standard theory of fracture mechanics and hydrology argue that this channel development would make difficult any continued expansion of the slipping zone. A crack ending in a channel has greatly diminished stress and strain rate concentration, and the high Terzaghi effective stress just outside the channel may stop the outward propagation of a slipping zone, that is, stop outward margin migration.

4. Discussion

4.1. Possible field evidence of temperate ice and channelized bed drainage at margin

Clarke et al. [2000] used a high power radar system to image the entire thickness of the Unicorn (Ridge B1-B2) ice sheet. They made profiles in multiple directions and found numerous linear diffractors near the base of the ice sheet. One special feature that was recognized is the occurrence of diffractors 230 m above the bed. These latter ones follow what they called the "Fishhook", a surface lineation observed in satellite imagery that is parallel to the north margin of Whillans ice stream B1 and located at the middle of Unicorn. One possible explanation mentioned of these features is that they reflect a zone of wet, temperate ice, that marks the inner boundary of an abandoned shear margin while the outer boundary is marked by a band of crevasses that used to be the band of arcuate crevasses (now observed at the outer boundary of Dragon margin). This supports the idea already invoked by *Jacobson and Raymond* [1998] that temperate ice is present at the margin over a substantial fraction of the sheet thickness due to intense shearing.

Clarke et al. [2000] also mentioned, citing a personal communication from H. Engelhardt, that a Caltech group had drilled into the ice at Unicorn approximately 1 km away of the outer boundary of the north margin of Whillans ice stream B1 (see Figure 6). They report that at $\sim$ 56 m above the bed the drill began encountering abnormal resistance. The penetration rate slowed significantly within layers at 56-49 m, 44-22 m and 14-0 m above the bed and some fresh scratches were observed on the the metal drill tip once back at the surface. They argue that these observations are strongly suggestive of entrained morainal debris. One of the possible mechanisms of formation of this debris is meltwater processes depositing sediment over a long period of time. We suggest that this such morainal debris is a plausible result of marginal channel development at the bed of the abandoned north shear margin of Whillans ice stream B1.

A borehole has been made at one shear margin of Kamb ice stream, the main stream of which stopped flowing $\sim$ 150 years ago [*Smith et al.*, 2002]. *Vogel et al.* [2005] drilled to the bottom of the ice sheet at the transition between the active upper part of Kamb ice stream and its stopped main truck, where the center stream velocity is 25 $m.yr^{-1}$ (see Figure 3). They penetrated a 1.6 m tall water-filled cavity between the bottom of the ice and the bed, a size of the same order of magnitude as our rough estimation of a semicircular channel collecting water from 100 km upstream at Dragon margin. Additional, videos from the bottom of this borehole showed horizontal acceleration of small solid particles sinking into the cavity, indicating a still active flow of water

within the cavity (the direction of flow was not reported). They estimated that the shear margin reconnected to the basal hydrological system $\sim$ 60 years ago. They argue that the formation of this 1.6 m tall-water-filled cavity is associated to the re-supply of basal water from areas of basal melting further upstream. This raises the possibility that the borehole fortuitously encountered a channel of the type that we conjecture. At minimum, it shows that channelized transport beneath an ice stream margin is a realistic possibility and implies that a source of liquid water must exist near the margin, although we lack data to test with our 1-D model the concept that internal melting is occurring there.

4.2. Ice advection at a margin

Echelmeyer and Harrison [1999] measured the transverse component of velocity that shows an inward component of velocity from the inter stream B1-B2 called Unicorn to the south edge of the Dragon margin (i.e., outward-facing from the crevassing zone) of about 2 m.yr^{-1} and an outward component from the inward-facing of the crevassing zone to the south edge of the Dragon margin also about 2 m.yr^{-1} (see their Figure 4b). This transverse motion of cold ice from the ridge and warm ice from the inner margin must affect the margin's thermal regime, although that is beyond the scope of our present study. The region showing these transverse velocity components is also associated with a short scale fluctuation in ice sheet thickness, which is neglected in this study when producing the profile of temperate ice height in Figure 7a and Figure 8.

4.3. Concentrated shear heating near freely-slipping to locked transition at bed

In this paper the shear heating along a column of ice at stream margins is treated with the assumption that the strain rate is uniform over depth, like in *Scambos et al.* [1994] and *Echelmeyer et al.* [1994], and the lateral shear stress only depends on temperature (cf. equation (12)). However at the margins' bed, the transition between slipping condition under the ice stream to locked ridges, frozen to the bed, defines an anti-plane shear crack whose surface is the base of the ice sheet beneath the stream and whose tips lie along the shear margins (see Figure 9). That induces high stress and strain rate concentrations near the margins which coincide with an enhanced shear heating rate [*Schoof*, 2004; *Jacobson and Raymond*, 1998]. Let $f > 0$ be the enhancement factor and r and θ be the 2-D cylindrical coordinates with a pole at the transition in basal slip condition at bed. We thus write the shear heating as

$$\tau_{lat}\dot{\gamma}_{lat} = 2f(r,\theta)A(T)^{-1/3}\left(\frac{\dot{\gamma}_{lat}}{2}\right)^{4/3} \qquad (31)$$

This concentrated shear heating should internally melt more ice, i.e., generate a wider temperate zone, than what our 1-D model predicts, although it is beyond the scope of this paper to fully quantify this process.

This anti-plane shear crack like feature induces stress singularities at the margins that lead to intense meltwater generation along the bed, which, we suggest, could cause marginal channelized drainage development in close proximity to the slipping to locked transition (cf. Figure 9).

5. Conclusion

We have examined, and found evidence supportive of, the hypothesis that Western Antarctic Siple Coast ice stream width is set by development of important internal melting, i.e., development of temperate ice conditions, within the ice sheet at the margins. We first find that the ice deformation-heating work at the margins, when incorporated in a standard 1-D vertical heat transfer analysis [*Zotikov*, 1986], typically predicts temperatures in excess of the melting temperature. We thus produced a still 1-D, but more refined thermal model of margins, with a full temperature dependence of ice properties and allowing for a temperate zone adjoining the bed. Using published ice sheet deformation and thickness data, this model predicts that nearly all active margins of Siple Coast ice streams are in a state of partial melt, with temperate ice being present over a fraction of the ice height. For the strain rate and sheet thickness given by *Joughin et al.* [2002], we find that respectively 4, 43, 36, 37 and 22 % of the ice height of the Mercer, Whillans, Whillans B1, Whillans B2 and MacAyeal ice stream margins is temperate. Although the strain rate they measured at Bindschadler ice stream is not enough to allow a temperate zone to develop, *Scambos et al.* [1994] found, farther downstream, a strain rate at the margins that would melt 55 % of the ice sheet thickness according to our model.

Within the temperate zone the continuous deformation generates internal meltwater which percolates toward the bed below in veins at triple junctions between ice grains. Using a strain rate profile made at the Dragon margin of Whillans ice stream B2, we find that the shear heating produces a basal meltwater rate of order of 10 mm.yr^{-1} over $\sim$ 2 km wide, approximatively the width of the chaotic crevassing zone that appears at this margin's surface. If this seeping meltwater at the margin's bed develops a channelized drainage of Röthlisberger type (R-channel) the accumulated seepage at the estimated rate at Dragon margin, if prevailing over 100 km upstream, is consistent with a semi-circular R-channel of 1.5 m diameter. We thus suggest that ice streams, existing at a width which corresponds to rapid internal melt generation, develop at the ice-till interface of their margins such channelized drainage.

We have proposed a possible related mechanism of stream's margin formation that is, of locking the ice sheet to the bed outboard of this R-channel. Indeed standard theory argues that the high, nearly lithostatic, pore pressure near the bed of fast flowing ice is somewhat alleviated within a channel. We find that the Terzaghi effective normal stress, pushing the ice sheet and till together and till particles into one another, is $\sim$ 100 times greater at the channel borders than what has been estimated under the rapidly moving central part of the ice stream, and locks the ice sheet to the bed. This transition between basal slipping under a stream and locked ridges at an ice sheet bed defines an anti-plane shear crack whose surface is the base of the ice sheet beneath the stream and whose tips lie along the shear margins. This crack strongly concentrates stress and strain rate near the shear margins. However, a crack ending in a channel, such as we predict at the margins, has greatly diminished stress and strain rate concentration, and the high Terzaghi effective normal stress just outside the channel makes difficult any continued expansion of the slipping. That locks the ice sheet to the bed outboard of the marginal channels and naturally forms an ice stream shear margin, as a limit to the fast-flowing ice.

However our 1-D vertical thermal modeling of temperate Siple Coast ice stream margins do not take into account the thermal effect of observed transverse motion of ice at margins which might be a result of the ice mass lost through the melting processes that we predict. From a modeling perspective, one would ultimately want to extend this analysis into (at least) 2-D, allowing transverse motion of ice at the margins and a shear heating concentration due to the basal sliding condition transition between slipping at ice stream bed and locked bed under the ridges.

Notation

a surface accumulation rate of ice, m.yr^{-1}.

A temperature-dependent creep parameter, $s^{-1}.Pa^{-3}$.

α_{th} thermal diffusivity of ice, $m^2.s^{-1}$.

B temperature-dependent creep parameter, $Pa.s^{1/3}$.

C_i ice specific heat, $J.kg^{-1}.K^{-1}$.

$\dot{\gamma}_{lat}$ lateral "engineering" shear strain rate, yr^{-1}.

f shear heating enhancement factor due to transition in basal slip condition, [1]

F perturbation factor of the ice creep strength due to the porosity, [1].

g acceleration due to gravity, $m.s^{-2}$.

G magnitude of the force per unit volume driving water flow in a conduit, $Pa.m^{-1}$.

G_0 Temperature gradient at the ice sheet base, $K.m^{-1}$.

H ice sheet thickness, m.

H' temperate height of ice, m.

k_{ice} ice permeability, m^2.

K ice thermal conductivity, $W.m^{-1}.K^{-1}$.

L latent heat per unit mass, $J.kg^{-1}$.

$\dot{m}$ melt rate per unit of volume, $kg.s^{-1}.m^{-3}$.

μ_w dynamic viscosity of water, Pa.s.

n volume of internal meltwater per unit of volume of ice, [1].

p water pore pressure, Pa.

P Péclet number, [1].

q_w vertical downward water Darcy flux, $m.s^{-1}$.

ρ_w density of water, $kg.m^{-3}$.

ρ_{ice} density of ice, $kg.m^{-3}$.

$T(z)$ vertical temperature profile, K.

T_{melt} basal melting temperature of ice, K.

T_{atm} atmospheric temperature, K.

t time, s.

τ_{lat} local lateral shear stress parallel to the downslope direction, Pa.

$\bar{\tau}_{lat}$ average of the lateral shear stress over the ice thickness, Pa.

τ_{grav} gravitational driving stress, Pa.

τ_{base} basal shear stress, Pa.

x downstream cartesian coordinate, m.

y cross-slope cartesian coordinate, m.

z cartesian coordinate measured perpendicularly to the bed, m.

v_m basal melt rate, $m.s^{-1}$.

w upward velocity measured perpendicularly to the bed, $m.s^{-1}$.

W ice stream width, m.

Φ volumetric rate of internal heat production, $W.m^{-3}$

Acknowledgments. This research was supported by the National Science Foundation through Office of Polar Programs grant ANT-0739444. The authors thank John Platt and Jenny Suckale for many discussions of the concepts and modeling techniques, thank Timothy Creyts for providing us with a comprehensive review of prior studies, Robert Viesca for comments on the manuscript, and also Garry Clarke, Ian Hewitt, Ian Joughin, Jean-Arthur Olive and Christian Schoof for fruitful discussions.

References

Brocq, A. L., A. Payne, M. Siegert, and R. Alley, A subglacial water-flow model for West Antarctica, *Journal of Glaciology*, *55*(193), 879–888, doi:10.3189/002214309790152564, 2009.

Clarke, T. S., C. Liu, N. E. Lord, and C. R. Bentley, Evidence for a recently abandoned shear margin adjacent to ice stream B2, Antarctica, from ice-penetrating radar measurements, *Journal of Geophysical Research*, *105*(B6), 2000.

Cuffey, K., and W. Paterson, *The Physics of Glaciers (Fourth Edition)*, ISBN 9780123694614, Elsevier, 2010.

Echelmeyer, K., and W. Harrison, Ongoing margin migration of Ice Stream B, Antarctica, *Journal of Glaciology*, *45*(150), 361–369, 1999.

Echelmeyer, K., W. Harrison, C. Larsen, and J. Mitchell, The role of the margins in the dynamics of an active ice stream, *Journal of Glaciology*, *40*(136), 527–538, 1994.

Flowers, G., and K. Clarke, A multicomponent coupled model of glacier hydrology 1. theory and synthetic examples, *Journal of Geophysical Research*, *107*(B11), doi:10.1029/2001JB001122, 2002.

Fricker, H. A., T. Scambos, S. Carter, C. Davis, T. Haran, and I. Joughin, Synthesizing multiple remote-sensing techniques for subglacial hydrologic mapping: application to a lake system beneath MacAyeal Ice Stream, West Antarctica, *Journal of Glaciology*, *56*(196), 187–199, doi:10.3189/002214310791968557, 2010.

Harrison, W., K. A. Echelmeyer, and C. Larsen, Measurement of temperature in a margin of Ice Stream B, Antarctica : implications for margin migration and lateral drag, *Journal of Glaciology*, *44*(148), 1998.

Hewitt, I. J., Modelling distributed and channelized subglacial drainage: the spacing of channels, *Journal of Glaciology*, *57*(202), 302–314, doi:10.3189/002214311796405951, 2011.

Jackson, M., and B. Kamb, The marginal shear stress of Ice Stream B, West Antarctica, *Journal of Glaciology*, *43*(145), 415–426, 1997.

Jacobson, H., and C. Raymond, Thermal effects on the location of ice stream margins, *Journal of Geophysical Research*, *103*(B6), 111–122, 1998.

Jordan, R., and J. Stark, Capillary Tension in Rotting Ice Laters, *Tech. rep.*, Technical Report ERDC/CRREL TR-01-13. US Army Corps of Engineers, Cold Regions Research and Engineering Laboratory, 2001.

Joughin, I., S. Tulaczyk, R. Bindschadler, and S. F. Price, Changes in West Antarctic Ice Stream velocities: Observation and analysis, *J. Geophys. Res.*, *107*(B11), doi:10.1029/2001JB001029, 2002.

Joughin, I., S. Tulaczyk, and H. Engelhardt, Basal melt beneath Whillans Ice Stream and Ice Streams A and C, West Antarctica, *Annals of Glaciology*, *36*, 257–262, doi:10.3189/172756403781816130, 2003.

Joughin, I., D. R. MacAyeal, and S. Tulaczyk, Basal shear stress of the Ross ice streams from control method inversions, *J. Geophys. Res.*, *109*(B9), doi:10.1029/2003JB002960, 2004a.

Joughin, I., S. Tulaczyk, D. R. MacAyeal, and H. Engelhardt, Melting and freezing beneath the Ross ice streams, Antarctica, *Journal of Glaciology*, *50*(168), 96–108, doi:10.3189/172756504781830295, 2004b.

Joughin, I., et al., Continued deceleration of whillans ice stream, west antarctica, *Geophys. Res. Lett.*, *32*(22), L22,501, doi:10.1029/2005GL024319, 2005.

Kamb, B., Basal zone of the West Antarctic Ice Streams and its role in lubrication of their rapid motion, in *The West Antarctic Ice Sheet: Behavior and Environment*, vol. 77, edited by R. B. Alley and R. A. Bindschadler, pp. 157–199, AGU, Washington, DC, doi:10.1029/AR077p0157, 2001.

Lliboutry, L., Temperate ice permeability, stability of water veins and percolation of internal meltwater, *Journal of Glaciology*, *42*(141), 201–211, 1996.

Nye, B. F., and F. C. Frank, Hydrology of the intergranular veins in a temperate glacier, *Journal of Glaciology*, 1973.

Nye, J., Water flow in glaciers: jökulhlaups, tunnels and veins, *Journal of Glaciology*, *17*(76), 181–207, 1976.

Nye, J., The geometry of water veins and nodes in polycrystalline ice, *Journal of Glaciology*, *35*, 17–22, 1989.

Perol, T., and J. R. Rice, Control of the width of West Antarctic ice streams by internal melting in the ice sheet near the margins, abstract C11B-0677 presented at 2011 Fall Meeting, AGU, San Francisco, Calif., 5-9 Dec., 2011.

Raymond, C., K. Echelmeyer, I. Whillans, and C. Doake, Ice stream shear margins, in *The West Antarctic Ice Sheet: Behavior and Environment*, vol. 77, pp. 137–55, American Geophysical Union, Antarctic Research Series, 2001.

Röthlisberger, H., Water pressure in intra- and subglacial channels, *Journal of Glaciology*, *11*(62), 177–203, 1972.

Scambos, T., K. Echelmeyer, M. Fahnestock, and R. Bindschadler, Develoment of enhanced ice flow at the southern margin of Ice Stream D, Antarctica, *Annals of Glaciology*, *20*, 313–318, 1994.

Schoof, C., On the mechanics of ice-stream shear margins, *Journal of Glaciology*, *50*(169), 208–218, doi:10.3189/172756504781830024, 2004.

Schoof, C., Ice-sheet acceleration driven by melt supply variability, *Nature*, *468*, doi:10.1038/nature09618, 2010.

Shabtaie, S., and C. Bentley, West Antarctic Ice Streams Draining into the Ross Ice Shelf: Configuration and Mass Balance, *Journal of Geophysical Research*, *92*, 1311–1336, 1987.

Smith, B., N. Lord, and C. Bentley, Crevasse ages on the northern margin of Ice Stream C, West Antarctica, *Annals of Glaciology*, *34*(1), 209–216, doi:10.3189/172756402781817932, 2002.

Tulaczyk, S., W. B. Kamb, and H. Engelhardt, Basal mechanics of Ice Stream B, West Antarctica 1. till mechanics, *Journal of Geophysical Research*, *105*(B1), 463–481, doi:10.1029/1999JB900329, 2000.

Van Der Veen, C., and I. Whillans, Model experiments on the evolution and stability of ice streams, *Annals of Glaciology*, *23*, 129–137, 1996.

Vaughan, D. G., and J. R. Spouge, Risk Estimation of Collapse of the West Antarctic Ice Sheet, *Climatic Change*, *52*, 65–91, doi:10.1023/A:1013038920600, 2002.

Vogel, S., The basal regime of the West-Antarctic Ice Sheet. interaction of subglacial geology with ice dynamics, Ph.D. thesis, University of California Santa Cruz, 2004.

Vogel, S. W., S. Tulaczyk, B. Kamb, H. Engelhardt, F. D. Carsey, A. E. Behar, A. L. Lane, and I. Joughin, Subglacial conditions during and after stoppage of an Antarctic Ice Stream: Is reactivation imminent?, *Geophysical Research Letter*, *32*, doi:10.1029/2005GL022563, 2005.

Whillans, I., and C. Van Der Veen, New and improved determinations of velocity of Ice Streams B and C, West Antarctica, *Journal of Glaciology*, 1993.

Zotikov, I., *The Thermophysics Of Glaciers*, D. Reidel, Mass, 1986.

Thibaut Perol, Department of Earth and Planetary Sciences, Harvard University, 327 Pierce Hall, 29 Oxford Street, Cambridge, MA 02138, USA. (thibaut.perol@post.harvard.edu)

James R. Rice, Department of Earth and Planetary Sciences and School of Engineering and Applied Sciences, Harvard University, 224 Pierce Hall, 29 Oxford Street, Cambridge, MA 02138, USA. (rice@seas.harvard.edu)

Appendix A: Analytical solution of the 1-D conduction-advection model with internal heating

To solve

$$\alpha_{th}\frac{\mathrm{d}^2T}{\mathrm{d}z^2}+\frac{az}{H}\frac{\mathrm{d}T}{\mathrm{d}z}+\frac{\tau_{lat}\dot{\gamma}_{lat}}{\rho_{ice}C_i}=0 \tag{A1}$$

let us define $G=(\mathrm{d}T/\mathrm{d}z)$, $\eta=(z/H)^2$, $S=\tau_{lat}\dot{\gamma}_{lat}$ and $P\equiv Pe=aH/\alpha$ the Péclet number. Then,

$$2\alpha_{th}\frac{\mathrm{d}G}{\mathrm{d}\eta}+aHG=-\frac{SH}{\rho_{ice}C}\frac{1}{\sqrt{\eta}} \tag{A2}$$

Ultimately we write

$$\frac{\mathrm{d}}{\mathrm{d}\eta}\left[G\exp(P\eta/2)\right]=-\frac{SH}{2\rho_{ice}C\alpha_{th}}\frac{1}{\sqrt{\eta}}\exp(P\eta/2) \tag{A3}$$

With $G_o=(\mathrm{d}T/\mathrm{d}z)_{z=0}$, integration gives

$$G\exp(P\eta/2)-G_o=-\frac{SH}{2\rho_{ice}C\alpha_{th}}\int_0^\eta\frac{1}{\sqrt{\eta}}\exp(P\eta/2)\,\mathrm{d}\eta \tag{A4}$$

so,

$$\begin{aligned}G &= G_o\exp(-Pz^2/2H^2)\\ &\quad -\frac{S}{K}\int_0^z\exp\left[-P(z^2-\tilde{z}^2)/2H^2\right]\mathrm{d}\tilde{z}\end{aligned} \tag{A5}$$

while

$$\int_0^z\exp(-Pz^2/2H^2)\,\mathrm{d}z=\frac{\sqrt{\pi}H}{2\sqrt{P/2}}\,\mathrm{erf}\left(\frac{\sqrt{P/2}\,z}{H}\right) \tag{A6}$$

Integration of equation (A5) using $T(z=0)=T_{melt}$ gives

$$\begin{aligned}T(z) &= T_{melt}+\sqrt{\frac{\pi}{2P}}HG_o\,\mathrm{erf}\left(\frac{\sqrt{P/2}\,z}{H}\right)\\ &\quad -\frac{S}{K_{avg}}\int_0^z\int_0^{\hat{z}}\exp\left[P(\tilde{z}^2-\hat{z}^2)/2H^2\right]\mathrm{d}\tilde{z}\mathrm{d}\hat{z}\end{aligned} \tag{A7}$$

Using polar coordinates in the integrations in the $z,\tilde{z}$ plane, the analytical temperature distribution along the z-axis is

$$\begin{aligned}T(z) &= T_{melt}+\sqrt{\frac{\pi}{2P}}HG_o\,\mathrm{erf}\left(\frac{\sqrt{P/2}\,z}{H}\right)\\ &\quad -\frac{SH^2}{K_{avg}P}\int_0^{\pi/4}\frac{1-\exp\left(-\frac{P\cos(2\theta)}{2\cos^2(\theta)}\frac{z^2}{H^2}\right)}{\cos(2\theta)}\,\mathrm{d}\theta\end{aligned} \tag{A8}$$

Rewriting the latter integral, the temperature profile along the z-axis is

$$\begin{aligned}T(z) &= T_{melt}+\sqrt{\frac{\pi}{2P}}HG_0\,\mathrm{erf}\left(\sqrt{P/2}\,\frac{z}{H}\right)\\ &\quad +\frac{\tau_{lat}\dot{\gamma}_{lat}H^2}{K_{avg}P}\int_0^1\frac{1-\exp\left(-\lambda Pz^2/2H^2\right)}{2\lambda\sqrt{1-\lambda}}\,\mathrm{d}\lambda\end{aligned} \tag{A9}$$

and G_o is found matching the second boundary condition $T(z=H)=T_{atm}$,

$$\begin{aligned}G_0 &= \frac{2\sqrt{P/2}}{\sqrt{\pi}H\,\mathrm{erf}\left(\sqrt{P/2}\right)}\left(T_{atm}-T_{melt}\right.\\ &\quad \left.-\frac{\tau_{lat}\dot{\gamma}_{lat}H^2}{K_{avg}P}\int_0^1\frac{1-\exp\left(-\lambda Pz^2/2H^2\right)}{2\lambda\sqrt{1-\lambda}}\,\mathrm{d}\lambda\right)\end{aligned} \tag{A10}$$

Appendix B: Thermally activated ice creep

The ice creep softening with increasing temperature could be described by an Arrhenius law with a switch of activation energy Q_c at a transition temperature $T^*=-10.6\,^\circ$C *Cuffey*

and Paterson [2010]. In our model the temperature dependency of the creep parameter A, as in $\dot{\gamma} = 2A(T)\tau^3$, follows

$$A(T) = A^* \exp\left(-\frac{Q_c}{R}\left[\frac{1}{T_h} - \frac{1}{T^*}\right]\right) \quad \text{(B1)}$$

where A^* is a pre-exponential constant and $R = 8.314$ J.K^{-1}.mol^{-1} is the gas constant. T_h is the temperature increased by a small term modeling the pressure dependence, $T_h/(\mathrm{K}) = T/(\mathrm{K})+0.6$, which is needed to fit the recommended values of the creep parameter based on results from field analyses and laboratory experiments (Table 3.4 in [*Cuffey and Paterson*, 2010]; values reported in Figure 10). We use an activation energy of $Q_c = 60$ kJ.mol^{-1} for $T_h < T^*$ and $Q_c = 115$ kJ.mol^{-1} for $T_h > T^*$ and $A^* = 3.5 \times 10^{-25}$ s^{-1}.Pa^{-3} (the value of A at -10 °C) as suggested by *Cuffey and Paterson* [2010]; $A(T)$ is depicted graphically in Figure 10. The creep parameter $B = A^{-1/3}$ at -0.6 °C, the basal melting point under some of our ice stream profiles (see Table 1), is 273 kPa.yr$^{1/3}$. It is about 60 % of its value at -10 °C; $B^* \equiv (A^*)^{-1/3} = 450$ kPa.yr$^{1/3}$. Thus the ice has the property of remaining strong even when temperate.

Additionally to the thermally activated creeping, one could model the softening due to intense shearing with an enhancement factor $E > 1$ as in $\dot{\gamma} = 2EA(T)\tau^3$. Since *Jackson and Kamb* [1997] did not find a strongly developed single maximum ice fabric even at a shear margin of a Siple Coast ice stream studying in this paper (the Dragon margin of Whillans ice stream B2), we choose to neglect this term in our analysis.

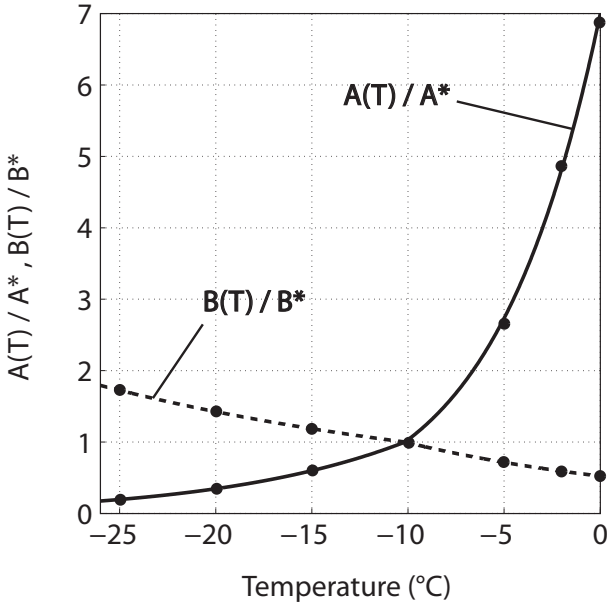

Figure 10. Arrhenius law followed by ice creep and used in our model; a switch of activation energy appears at a transition temperature $T^* = -10.6$ °C. The black circles represent the recommended values of the creep parameters A and $B = A^{-1/3}$ by *Cuffey and Paterson* [2010] which fit results from field analyses and laboratory experiments.